# Pulled Polymer Loops as a Model for the Alignment of Meiotic Chromosomes

Yen Ting Lin,[1] Daniela Frömberg,[1] Wenwen Huang,[1] Petrina Delivani,[2] Mariola Chacón,[2] Iva M. Tolić,[2,3]
Frank Jülicher,[1] and Vasily Zaburdaev[1]

[1]*Max Planck Institute for the Physics of Complex Systems, Nöthnitzer Straße 38, D-01187 Dresden, Germany*
[2]*Max Planck Institute of Molecular Cell Biology and Genetics, Pfotenhauerstrasse 108, D-01307 Dresden, Germany*
[3]*Division of Molecular Biology, Ruđer Bošković Institute, Bijenička cesta 54, 10000 Zagreb, Croatia*

During recombination, the DNA of parents exchange their genetic information to give rise to a genetically unique offspring. For recombination to occur, homologous chromosomes need to find each other and align with high precision. Fission yeast solves this problem by folding chromosomes in loops and pulling them through the viscous nucleoplasm. We propose a theory of pulled polymer loops to quantify the effect of drag forces on the alignment of chromosomes. We introduce an external force field to the concept of a Brownian bridge and thus solve for the statistics of loop configurations in space.

The process of meiosis lies at the origin of genetic diversity in nature and is the starting point of gamete formation [1]. In meiosis, homologous chromosomes are brought in close physical proximity to exchange genetic information in a process known as recombination [1–3]. For recombination to occur, homologous chromosomes need to align and pair up. Pairing is a complex event that involves the association of homologous loci, the formation of protein complexes, and the local remodeling of the DNA such as double-strand breaks [4]. Our goal is to elucidate the role of viscous forces in the alignment of chromosomes during meiosis in fission yeast.

Fission yeast *Schizosaccharomyces pombe* (*S. pombe*) is a model organism in cell biology and for studying meiosis [5–8]. Upon starvation, two cells of opposing mating types can fuse and proceed to meiosis. Its initial stage is marked by an extended phase of nuclear oscillations where the whole nucleus is dragged from one pole of the elongated zygote to the other [see Fig. 1(a) and Movie S1 in the Supplemental Material [9]]. Oscillations have a period of about 10 min and can last for up to 3 h. It was shown that microtubules and dynein motors drive these oscillations [15–19]. The exact role of this dramatic nuclear movement, however, remains unclear [20]. It was suggested that nuclear movements help to align chromosomes before they may proceed to pairing and recombination [21,22]. Experimental data show that the distance between two homologous loci gradually decreases during the oscillations until they pair and, conversely, if oscillations are stopped the loci remain far apart and fail to pair [21]. This observation underlines the importance of understanding the physical mechanisms that govern the alignment of the chromosomes preceding the recombination.

In fission yeast, three pairs of chromosomes are bound by both ends to the spindle pole body (SPB), which is at the same time the anchoring point of growing microtubules,

see Fig 1(b). Under the force generated by molecular motors anchored to the cell cortex and pulling on microtubules, the SPB drags the nuclear envelope and the chromosomes inside. A possible physical mechanism for the alignment of chromosomes is that viscous drag stretches the chromosomes in a loop geometry thus reducing the distance between homologous loops. This has a metaphoric similarity to doing washing in a river. In this Letter, we investigate how the drag force affects the spatial configuration of pinned polymer loops and how it enhances their contact probability. Remarkably, within the same framework we can take into account additional constraints, such as newly formed recombination spots. To address these problems we use the ubiquitous freely jointed chain model of a polymer [23].

*Model.*—We represent the chromosome by a chain of beads connected with $N$ freely jointed rods, where the length of a rod $a$ is given by the Kuhn length of the chromatin fiber. Here, we focus on the quasistationary phase of the oscillations when the SPB is pulled with an almost constant speed $v_0$ [16] from one pole of the elongated cell to the other. For simplicity, we approximate the trajectory of the SPB by a straight line.

As the chromosomes are pulled through the nucleoplasm they experience a friction force. In the comoving frame of reference associated with the SPB, the relative motion of the fluid with constant speed results, in our model, in the constant force $|\mathbf{F}| = \gamma v_0$ acting on every bead, where $\gamma$ is an isotropic Stokes friction coefficient, Fig. 1(c). The force points in the positive direction of the $z$ axis. We identify the first and last beads of the chain with the SPB, thereby closing the chain to a loop. In the comoving frame these beads do not move. In addition to regular forces there is a stochastic component resulting from thermal fluctuations but also from other active but intrinsically random processes within the cell, such as the activity of molecular
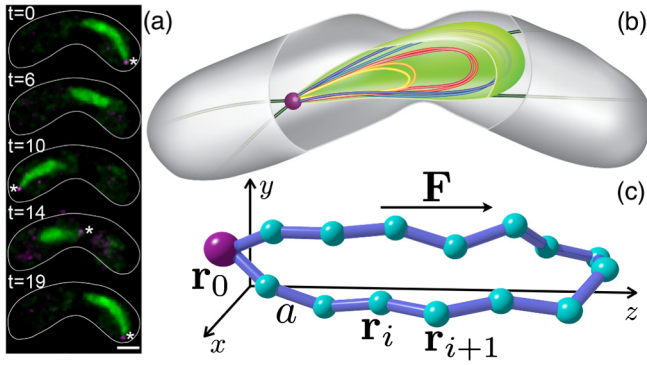
FIG. 1 (color online).    From meiotic oscillations to the polymer loop model. (a) Sequential images of the moving chromatin and the spindle pole body (asterisks) during the horsetail oscillation phase of meiosis in fission yeast [9]. The scale bar is 2 $\mu$m; time is given in minutes. (b) Sketch of the cell during oscillations. Both ends of each chromosome are bound to the SPB and form loops. The SPB is pulled by multiple dynein motors (not shown) walking along microtubules. The SPB is anchored to the nuclear envelope and entrains the whole nucleus. (c) The polymer loop as a bead-rod chain. A uniform force field **F** points in $z$ direction. Beads are numbered by index $i$, have positions $\mathbf{r}_i$, and are connected by rods of length $a$. The loop is pinned at the location of the SPB, $\mathbf{r}_0 = 0$.

motors or transcription. For simplicity we characterize these by an effective temperature $T$, which is assumed to be uniform along the chromosomes [24]. Our goal is to describe the statistics of a pinned polymer loop as a function of a constant uniform force and the noise level. To solve this inherently nonequilibrium problem we make use of the following mapping to an equilibrium setting.

We denote the position of each bead as $\mathbf{r}_i$, $i \in [0, N]$, and $\mathbf{r}_0 = \mathbf{r}_N = 0$ is the loop condition. The potential energy of the chain is

$$U = U_0 - a \sum_{i=1}^{N} \sum_{j=1}^{i} \mathbf{F} \mathbf{e}_j, \qquad \mathbf{e}_j = \frac{1}{a}(\mathbf{r}_j - \mathbf{r}_{j-1}), \quad (1)$$

where $U_0$ is a constant and we used the equality $\mathbf{r}_i = a \sum_{j=1}^{i} \mathbf{e}_j$. We are interested in the marginal distribution of the $i$th bead at equilibrium, which is determined by the potential energy of each polymer configuration and is a function of force and fluctuations.

*Force free regime: Brownian bridge solution.*—Without the external force our problem is similar to the Brownian bridge setup [25–27], a random walk in space that returns to the starting point after $N$ steps, where the role of time is played by the distance measured along the trajectory. From all random walk paths of length $N$ we select only those that return to the origin. The positional probability density function (PDF) of the $i$th bead on the loop $\rho^L(\mathbf{r}_i = \mathbf{r})$ can be found by noting that there have to be two trajectories with $i$ and $N - i$ steps, respectively, leading to the same

point **r**. The probability of this event is normalized by the probability of the trajectory with $N$ steps to form a loop:

$$\rho^L(\mathbf{r}_i = \mathbf{r}) = \frac{\rho(\mathbf{r}_i = \mathbf{r}|\mathbf{r}_0 = 0)\rho(\mathbf{r}_{N-i} = \mathbf{r}|\mathbf{r}_0 = 0)}{\rho(\mathbf{r}_N = 0|\mathbf{r}_0 = 0)}. \quad (2)$$

Here, $\rho(\mathbf{r}_k = \mathbf{r}|\mathbf{r}_0 = 0)$ is the propagator of the corresponding random walk process. In the case of the random chain model, the orientation of each rod is independent and random, and therefore for $k \gg 1$, $\rho(\mathbf{r}_k = \mathbf{r}|\mathbf{r}_0 = 0)$ is a Gaussian distribution with a zero mean and a variance that is a sum of the variances of all individual steps. As a result, $\rho^L(\mathbf{r}_i = \mathbf{r})$ is also Gaussian with a zero mean and a variance that is given by

$$\sigma_i^2 = \frac{\sigma_{0 \to i}^2 \sigma_{0 \to N-i}^2}{\sigma_{0 \to N}^2}. \quad (3)$$

Here, $\sigma_{0 \to k}^2 = a^2 k$ is the variance accumulated on the path from the origin to bead $k$. Therefore, the fluctuations of the position of a bead with an index $i$ are described by $\langle \mathbf{r}_i^2 \rangle = a^2 i(N - i)/N$ [25,26]; they are maximal at the midpoint of the loop, $i = N/2$, and vanish when approaching the pinned point $i = \{0, N\}$. If an external force is applied to each bead, it affects the orientation of the connecting rods and therefore changes the statistics of the whole chain.

*Brownian bridge with an external force.*—We rewrite the potential energy (1) using spherical coordinates with the $z$ axis pointing in the direction of the force and $\theta_i$ denoting the angle between the $i$th rod and the $z$ axis. By exchanging the summation order in Eq. (1) and using the loop condition for the $z$ projections of the rods $\sum_{i=1}^{N} ae_{i,z} = a \sum_{i=1}^{N} \cos \theta_i = 0$ we arrive at

$$U = \tilde{U}_0 + \gamma a v_0 \sum_{j=1}^{N} j \cos \theta_j. \quad (4)$$

To determine the statistical properties of the orientation of the rods we use the grand-canonical partition function

$$Z = \prod_j Z_j = \prod_j \int_0^{2\pi} d\phi \int_0^{\pi} d\theta \sin\theta \exp\left(-\frac{(j-\mu)\cos\theta}{2\tilde{T}}\right), \quad (5)$$

where we introduced the rescaled temperature $\tilde{T} = k_B T / 2\gamma a v_0$. The chemical potential $\mu$ plays the role of a Lagrange multiplier and will be determined below. The partition function $Z_j$ can be calculated as

$$Z_j = \frac{2\tilde{T} \sinh\frac{(j-\mu)}{2\tilde{T}}}{j - \mu}. \quad (6)$$

We then compute the mean and variance of $\cos\theta_j$

$$\langle\cos\theta_j\rangle = 2\tilde{T}\partial_\mu \ln Z_j = \coth\frac{\mu-j}{2\tilde{T}} - \frac{2\tilde{T}}{\mu-j},$$

$$\mathrm{var}[\cos\theta_j] = 4\tilde{T}^2\partial_\mu^2 \ln Z_j = \frac{4\tilde{T}^2}{(j-\mu)^2} - \mathrm{csch}^2\frac{j-\mu}{2\tilde{T}}. \quad (7)$$

By using the loop condition $a\sum_{i=1}^{N}\langle\cos\theta_j\rangle = 0$ we determine the chemical potential $\mu = (N+1)/2$. For symmetry reasons, the remaining two average projections of the rod are zero: $\langle e_{j,x}\rangle = \langle e_{j,y}\rangle = 0$. The fixed length of the rod connects fluctuations orthogonal and parallel to the force $\langle e_{j,x}^2\rangle = \langle e_{j,y}^2\rangle = (1 - \langle\cos^2\theta_j\rangle)/2$.

This gives us the statistical properties of the orientations of the individual rods [28]. The covariance matrix of each individual rod orientation is diagonal due to the azimuthal symmetry. In this case, according to the multivariate Lindeberg-Feller central limit theorem [29,30], the PDF of the bead position after summing the contributions of many individual rods is a multivariate Gaussian. For example, for the propagator in the $z$ direction we have (for $k \gg 1$) a Gaussian distribution with the following mean and variance:

$$\langle z_k\rangle = a\sum_{j=1}^{k}\langle\cos\theta_j\rangle, \quad \sigma_{0\to k,z}^2 = a^2\sum_{j=1}^{k}\mathrm{var}[\cos\theta_j]. \quad (8)$$

Importantly, these propagators produce random walk paths that return to zero only on average, similarly to unbiased random walk paths in the force-free case. To make sure that the chain returns to the origin exactly and to describe the fluctuations of the looped polymer chain we enforce the Brownian bridge condition (2). So for the $z$ axis we compute the fluctuations in the position of a bead belonging to a loop by substituting Eq. (8) into Eq. (3). This analytical result is in agreement with 3D Brownian dynamics simulations of the bead-rod model, see Fig. 2(a) and Ref. [9]. Fluctuations are decreasing for increasing force and, interestingly, their magnitudes are different in the directions along and orthogonal to the force, see Fig. S1 [9].

We can now quantify the relative separation of two similar loops. Because of the Gaussian statistics of a single loop, the relative distance between the two "homologous" beads on independent loops also has a Gaussian distribution. It has a zero mean, its variance is double the variance of the bead's position in a single loop, and the fluctuations in the $x$, $y$, and $z$ directions need to be summed up. Figure 2(b) shows how the fluctuations in the relative distance change with temperature where each line corresponds to a different position of a bead on the loop.

*Two intersecting loops.*—A recombination spot between two chromosomes forms a tight physical bond, thus reducing the relative fluctuations and facilitating further recombination events [7]. In fission yeast, there is another possible mechanism to form a bond between chromosomal
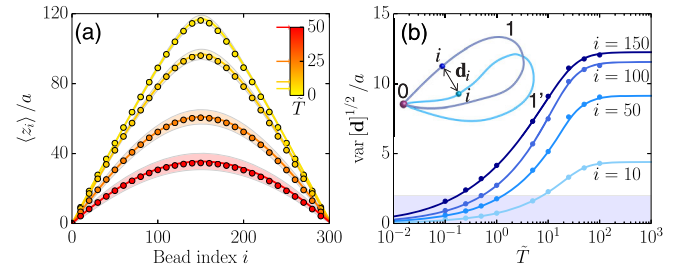


FIG. 2 (color online). Configurations of the loops in 3D. (a) Average positions of beads in the direction of the force of a single loop at different effective temperatures: theory (lines) and Brownian dynamics simulations (circles). Shaded regions show the corresponding square root of the variance (see also Fig. S1 [9]). (b) Fluctuations of the three-dimensional separation between two beads with the same index $i$ but belonging to two different loops (see the sketch in the inset) as a function of temperature. $i = 150$ corresponds to the middle of the loop. Fluctuations are decreasing for decreasing temperature and for beads closer to the pinned point. The shaded region denotes the separation below which the chromosomes are considered to be paired. For $a = 200$ nm this separation corresponds to 400 nm.

loops. Centromeres (located close to the midpoints of chromosomes) were suggested to have a high binding affinity to each other [21], thus providing an additional constraint point where the fluctuations are maximal. We can further generalize the model of the Brownian bridge with an external force to describe the statistics of two loops (denoted by 1 and $1'$) that have an additional constraint at some intermediate bead position with index $c$, see Fig. 3(a).

We redefine the loops as shown in Fig. 3(a). Loop $A$ starts at the pinned point, continues along loop 1, to the constraint point $c$, and then returns to the origin along loop $1'$ by the path of the same length. Loop $B$ joins the remaining pieces of the original loops 1 and $1'$. The statistics of each individual rod orientation in loops $A$ or $B$ is, however, defined by the parent loops 1 and $1'$. Let us focus on loop $A$ and quantify
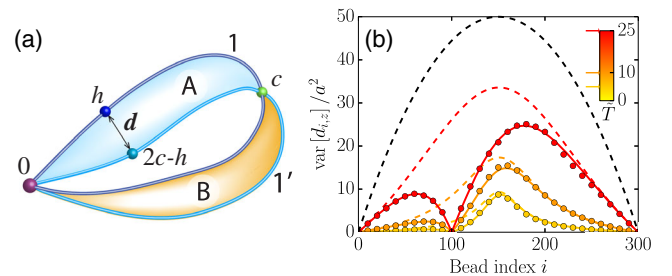


FIG. 3 (color online). Two loops with an additional constraint. (a) Two loops 1 and $1'$ are connected at one additional bead with index $c$. Shaded regions indicate the redefined loops $A$ and $B$. The separation **d** between two homologous beads can be calculated on the new loop $A$. (b) Fluctuations of the separation in the $z$ direction between homologous beads of the loops for different temperatures (circles and solid lines) compared to the unconstrained case (dashed lines). The constraint is located at the bead $i = 100$. The upper dashed line shows the limit of the unconstrained force-free Brownian bridge.

the relative separation $\mathbf{d}_h$ between two homologous beads with indices $h$ and $2c - h$, respectively. The PDF of $\mathbf{d}_h = (\mathbf{r}_h - \mathbf{r}_{2c-h})$ can be defined as

$$\rho(\mathbf{d}_h) = \langle \delta(\mathbf{d}_h - (\mathbf{r}_h - \mathbf{r}_{2c-h})) \rangle_{\mathbf{r}_h, \mathbf{r}_{2c-h}}, \qquad (9)$$

where we average over all possible spatial positions of two homologous beads. For that we use their joint positional PDF $\rho_{h,2c-h}(\mathbf{r}_1, \mathbf{r}_2)$ obtained similarly to Eq. (2):

$$\rho_{h,2c-h}(\mathbf{r}_1, \mathbf{r}_2) = \frac{\rho_{0 \to h}(\mathbf{r}_1|0)\rho_{h \to 2c-h}(\mathbf{r}_1|\mathbf{r}_2)\rho_{0 \to 2c-h}(\mathbf{r}_2|0)}{\rho_{0 \to 2c}(0|0)}. \qquad (10)$$

This is a probability density of three pieces of trajectory to connect two points, provided they belong to the same loop. Here, $\rho_{k \to j}(\mathbf{r}_1|\mathbf{r}_2)$ is the propagator of the random walk from bead $k$ to bead $j$. To find $\rho(\mathbf{d}_h)$ we rewrite Eq. (9) as an averaging integral:

$$\rho(\mathbf{d}_h) = \int \int d\mathbf{r}_1 d\mathbf{r}_2 \delta(\mathbf{d}_h - (\mathbf{r}_1 - \mathbf{r}_2))\rho_{h,2c-h}(\mathbf{r}_1, \mathbf{r}_2). \qquad (11)$$

This integral is easy to evaluate, as every propagator entering Eq. (11) is a (multivariate) Gaussian with a mean and a variance determined by the corresponding parts of the polymer loops contributing to it, as in Eq. (8). As a result the distribution of $\mathbf{d}_h$ is also Gaussian and, for example, its $z$ component has the variance

$$\text{var}[d_{h,z}] = 2\frac{\sigma_{0 \to h,z}^2 \sigma_{h \to c,z}^2}{\sigma_{0 \to c,z}^2}. \qquad (12)$$

We see that fluctuations of the distance disappear at the constraint point [$z = c$ in Eq. (12)], and reduce the overall distance between the two loops 1 and $1'$ as compared to the unconstrained case, see Fig. 3(b).

*Discussion.*—We can use our analytical results to calculate the force required to bring the chromosomes to a pairing distance and compare it to the forces estimated experimentally. The pairing distance is a separation between the homologous chromosomes that enables the molecular machinery of recombination to work [31]. In practice, due to the resolution limitation of fluorescence microscopy, two labeled homologous loci cannot be distinguished at a distance of 350–400 nm [21,31,32], thus setting an upper bound in estimating the pairing distance. As an example we consider the case when fluctuations fall below 400 nm. Using Fig. 2(b), which for the Kuhn length $a = 200$ nm and $N = 300$ describes the longest *S. pombe* chromosome, we find that the required rescaled temperature is about $\tilde{T} \approx 0.13$. From its definition, $\tilde{T} = k_B T/(2aF)$, and by considering thermal fluctuations, the friction force acting on each bead is $F \approx 8 \times 10^{-14}$ N.

This force value can be used to roughly estimate the nucleoplasmic viscosity. Using the Stokes relation

$F = 6\pi\eta Rv$, with the velocity $v \approx 2.5$ $\mu$m/min of the SPB [16], and a bead radius estimated by a persistence length $R \approx 100$ nm, we obtain $\eta \approx 0.64$ Pa $\cdot$ s. This value is larger than that reported for higher eukaryotic cells, 0.2–0.28 Pa $\cdot$ s [33,34], but smaller than the value 2.6 Pa $\cdot$ s previously found for *S. pombe* on the basis of measurements of microtubule diffusion [35]. This difference might result from the dependence of the measured viscosity on the size of the probe particle [35].

The total force required to pull three pairs of chromosomes is estimated in our model as $F_{\text{total}} = FN_{\text{total}}$, where $N_{\text{total}}$ is the total number of beads. For a Kuhn length of 200 nm [36–39], a compaction ratio of 100 bp/nm [40], and the nucleotide number 12.6 Mbp in *S. pombe* chromosomes [5], we have $\sim$1260 beads representing three pairs of chromosomes. This implies the total pulling force $F_{\text{total}} \approx 100$ pN. The stall force of dynein motors has been reported within the range of 1–7 pN [41,42]. The total force then corresponds to 14–100 dynein motors pulling together. This is consistent with previous measurements reporting 50–100 dynein motors engaged in pulling of the SPB [19]. Thus, the experimentally observed number of dynein motors can generate a force that, in the steady state regime of the model, would lead to the alignment of the chromosomes. We can use numerical simulations to estimate how fast a polymer loop reaches its steady-state regime under the action of the force. After the initial stretching during $\sim$12 min, the relaxation time to the steady state is of the order of 3 min (see Fig. S2 [9]), which is less than one period of the oscillations, thus supporting the relevance of the steady-state approximation.

To conclude, our results suggest that a rather simple, physical mechanism governs the alignment of chromosomes during meiosis in fission yeast. This alignment is an important prerequisite for successful chromosome pairing and recombination. The statistical model of pulled polymer loops provides a general theoretical framework for a broader class of polymer systems. Our results may help to design *in vitro* experiments on driven DNA loops to study recombination, and may also apply to bacterial DNA plasmids subjected to external fields and multilooped mitotic chromosomes and sister chromatids [43,44]. The study of the dynamics of pulled polymer loops will be an interesting and challenging problem for future research.

[1] B. Alberts, A. Johnson, J. Lewis, M. Raff, K. Roberts, and P. Walter, *Molecular Biology of the Cell*, 4th ed. (Garland Science, New York, 2002).

[2] J. L. Gerton and R. S. Hawley, Nat. Rev. Genet. **6**, 477 (2005).

[3] A. M. Villeneuve and K. J. Hillers, Cell **106**, 647 (2001).
[4] B. D. McKee, BBA-Gene. Struct. Expr. **1677**, 165 (2004).
[5] R. Egel, *The Molecular Biology of Schizosaccharomyces pombe: Genetics, Genomics and Beyond* (Springer, Berlin-Heidelberg, 2004).
[6] L. Davis and G. R. Smith, Proc. Natl. Acad. Sci. U.S.A. **98**, 8395 (2001).
[7] P. Munz, Genetics **137**, 701 (1994).
[8] J. L. Wells, D. W. Pryce, and R. J. McFarlane, Yeast **23**, 977 (2006).
[9] See Supplemental Material at http://link.aps.org/supplemental/10.1103/PhysRevLett.115.208102, which includes Refs. [10–14], for a detailed description of experimental procedures and numerical simulations.
[10] C. Cruz, F. Chinesta, and G. Régnier, Arch. Comput. Methods Eng. **19**, 227 (2012).
[11] E. Hinch, J. Fluid Mech. **271**, 219 (1994).
[12] M. Pasquali and D. C. Morse, J. Chem. Phys. **116**, 1834 (2002).
[13] M. Somasi, B. Khomami, N. J. Woo, J. S. Hur, and E. S. Shaqfeh, J. Non-Newtonian Fluid Mech. **108**, 227 (2002).
[14] T. W. Liu, J. Chem. Phys. **90**, 5826 (1989).
[15] D.-Q. Ding, Y. Chikashige, T. Haraguchi, and Y. Hiraoka, J. Cell Sci. **111**, 701 (1998).
[16] S. K. Vogel, N. Pavin, N. Maghelli, F. Jülicher, and I. M. Tolić-Nørrelykke, PLoS Biol. **7**, e1000087 (2009).
[17] A. Yamamoto, C. Tsutsumi, H. Kojima, K. Oiwa, and Y. Hiraoka, Mol. Biol. Cell **12**, 3933 (2001).
[18] A. Yamamoto, R. R. West, J. R. McIntosh, and Y. Hiraoka, J. Cell Biol. **145**, 1233 (1999).
[19] V. Ananthanarayanan, M. Schattat, S. K. Vogel, A. Krull, N. Pavin, and I. M. Tolić-Nørrelykke, Cell **153**, 1526 (2013).
[20] R. Koszul and N. Kleckner, Trends Cell Biol. **19**, 716 (2009).
[21] D.-Q. Ding, A. Yamamoto, T. Haraguchi, and Y. Hiraoka, Dev. Cell **6**, 329 (2004).
[22] D. J. Wynne, O. Rog, P. M. Carlton, and A. F. Dernburg, J. Cell Biol. **196**, 47 (2012).
[23] M. Doi and S. Edwards, *The Theory of Polymer Dynamics*, International Series of Monographs on Physics (Clarendon Press, Oxford, 1986).
[24] Since the recombination machinery, locally altering the properties of the chromatin, becomes active only after the homologous chromosomes come to close proximity, we assume the effective temperature to be spatially uniform.
[25] D. Revuz and M. Yor, *Continuous Martingales and Brownian Motion, Grundlehren der mathematischen Wissenschaften* (Springer, Berlin-Heidelberg, 1999).
[26] L. Rogers and D. Williams, *Diffusions, Markov Processes, and Martingales: Volume 1, Foundations,* Cambridge Mathematical Library (Cambridge University Press, Cambridge, 2000).
[27] S. N. Majumdar and A. Comtet, Phys. Rev. Lett. **92**, 225501 (2004).
[28] Interestingly, it can be shown that the statistics of rod orientations in a one-dimensional case is given by the Fermi-Dirac distribution. This problem will be discussed in detail elsewhere.
[29] W. Greene, *Econometric Analysis* (Prentice Hall, Upper Saddle River, NJ, 2008).
[30] K. Athreya and S. Lahiri, *Measure Theory and Probability Theory*, Springer Texts in Statistics (Springer, New York, 2006).
[31] D. Zickler and N. Kleckner, Annu. Rev. Genet. **33**, 603 (1999).
[32] G. A. Cromie, R. W. Hyppa, A. F. Taylor, K. Zakharyevich, N. Hunter, and G. R. Smith, Cell **127**, 1167 (2006).
[33] W. F. Marshall, J. F. Marko, D. A. Agard, and J. W. Sedat, Curr. Biol. **11**, 569 (2001).
[34] S. P. Alexander and C. L. Rieder, J. Cell Biol. **113**, 805 (1991).
[35] I. Kalinina, A. Nandi, P. Delivani, M. R. Chacón, A. H. Klemm, D. Ramunno-Johnson, A. Krull, B. Lindner, N. Pavin, and I. M. Tolić-Nørrelykke, Nat. Cell Biol. **15**, 82 (2013).
[36] K. Bystricky, P. Heun, L. Gehlen, J. Langowski, and S. M. Gasser, Proc. Natl. Acad. Sci. U.S.A. **101**, 16495 (2004).
[37] Y. Cui and C. Bustamante, Proc. Natl. Acad. Sci. U.S.A. **97**, 127 (2000).
[38] J. Langowski, Eur. Phys. J. E **19**, 241 (2006).
[39] A. Rosa and R. Everaers, PLoS Comput. Biol. **4**, e1000153 (2008).
[40] D.-Q. Ding, N. Sakurai, Y. Katou, T. Itoh, K. Shirahige, T. Haraguchi, and Y. Hiraoka, J. Cell Biol. **174**, 499 (2006).
[41] A. Gennerich, A. P. Carter, S. L. Reck-Peterson, and R. D. Vale, Cell **131**, 952 (2007).
[42] S. Toba, T. M. Watanabe, L. Yamaguchi-Okimoto, Y. Y. Toyoshima, and H. Higuchi, Proc. Natl. Acad. Sci. U.S.A. **103**, 5741 (2006).
[43] Y. Zhang and D. W. Heermann, PLoS One **6**, e29225 (2012).
[44] Y. Zhang, S. Isbaner, and D. W. Heermann, Front. Phys. **1**, doi:10.3389/fphy.2013.00016 (2013).